



# Evidence of icosahedral short-range order in Zr<sub>70</sub>Cu<sub>30</sub> and Zr<sub>70</sub>Cu<sub>29</sub>Pd<sub>1</sub> metallic glasses

著者	才田 淳治
journal or publication title	Applied Physics Letters
volume	83
number	19
page range	3924-3926
year	2003
URL	<a href="http://hdl.handle.net/10097/47500">http://hdl.handle.net/10097/47500</a>

doi: 10.1063/1.1626266

# Evidence of icosahedral short-range order in $\text{Zr}_{70}\text{Cu}_{30}$ and $\text{Zr}_{70}\text{Cu}_{29}\text{Pd}_1$ metallic glasses

K. Saksli, H. Franz, P. J  v  ri, K. Klementiev, E. Welter, and A. Ehnes  
HASYLAB at DESY, Notkestrasse 85, 22607 Hamburg, Germany

J. Saida  
Center for Interdisciplinary Research, Tohoku University, Sendai 980-8578, Japan

A. Inoue  
Institute for Materials Research, Tohoku University, Sendai 980-8577, Japan

J. Z. Jiang<sup>a)</sup>  
Department of Materials Science and Engineering, Zhejiang University, Hangzhou, 310027,  
People's Republic of China and Department of Physics, Building 307, Technical University of Denmark,  
DK-2800 Lyngby, Denmark

(Received 23 June 2003; accepted 18 September 2003)

Change in local atomic environment during crystallization of Zr-based glassy alloys was studied by extended x-ray absorption fine structure (EXAFS) spectroscopy. The formation of icosahedral quasicrystalline phase followed by crystallization of tetragonal  $\text{CuZr}_2$  has been observed in the  $\text{Zr}_{70}\text{Cu}_{29}\text{Pd}_1$  glassy alloy during annealing up to 850 K. On the other hand, the binary  $\text{Zr}_{70}\text{Cu}_{30}$  alloy shows a single glassy to crystalline  $\text{CuZr}_2$  phase transformation. The local atomic environment of as-quenched  $\text{Zr}_{70}\text{Cu}_{30}$  alloy is matched to an icosahedral local atomic configuration, which is similar to that of the as-quenched  $\text{Zr}_{70}\text{Cu}_{29}\text{Pd}_1$  alloy and the alloy annealed at 593 K containing icosahedral phase. Considering that the supercooled liquid region appears prior to crystallization in the  $\text{Zr}_{70}\text{Cu}_{30}$  glassy alloy, the observed results support the theory claiming a strong correlation between the existence of local icosahedral short-range order and stability of the supercooled liquid state.

   2003 American Institute of Physics. [DOI: 10.1063/1.1626266]

Recently, after the discovery of the formation of icosahedral quasicrystals (I-phase) from Zr-Al-Cu-Ni metallic glasses with high oxygen content,<sup>1</sup> quasicrystals have been found to form upon crystallization in many Zr-based alloy systems, such as Zr-(Pd or Pt),<sup>2-4</sup> Zr-Ni-(Pd, Au, Pt or Ti),<sup>5,6</sup> Zr-Cu-Al-O,<sup>7</sup> Zr-Pd-(Cu, Fe or Co),<sup>8,9</sup> Zr-Cu-Pd-(Al or Ni),<sup>8</sup> Zr-Al-Ni-Cu-O,<sup>1,10</sup> Zr-Al-Ni-(Pd, Au, or Pt),<sup>11</sup> Zr-Cu-Ti-Ni,<sup>12</sup> Zr-Al-Ni-Cu-(Ti, Au, Pt, Pd or Ag),<sup>13-18</sup> Zr-Ti-Cu-Ni-Be,<sup>19</sup> and Zr-Ti-Nb-Cu-Ni-Al.<sup>20</sup> Very recently, the formation of I-phase was reported in the binary  $\text{Zr}_{70}\text{Cu}_{30}$  glassy alloy after addition of 1 at. % Pd, Au or Pt.<sup>21</sup> Because the nanometer-sized I-phase is formed as a primary metastable phase by substituting only 1 at. % Cu with Pd in  $\text{Zr}_{70}\text{Cu}_{30}$ , Saida *et al.* suggested that icosahedral short- and/or medium-range order could already exist in the  $\text{Zr}_{70}\text{Cu}_{30}$  glassy alloy.<sup>22</sup> In this letter, we report evidence of the existence of icosahedral short-range order by examining the local environments of the  $\text{Zr}_{70}\text{Cu}_{30}$  and  $\text{Zr}_{70}\text{Cu}_{29}\text{Pd}_1$  glassy alloys in the as-quenched and annealed states using the extended x-ray absorption fine structure (EXAFS) technique.

Melt-spun  $\text{Zr}_{70}\text{Cu}_{30}$  binary and  $\text{Zr}_{70}\text{Cu}_{29}\text{Pd}_1$  ternary alloys with a cross section of  $0.03 \times 1 \text{ mm}^2$  were produced from ingots prepared by arc melting high-purity metals (99.9% Zr, 99.999% Cu, 99.9% Pd). The ternary alloy has been prepared by substituting Pd for 1 at. % Cu. Amorphous ribbons were obtained from these alloys by single-roller

melt spinning at a wheel surface velocity of 40 m/s in purified Ar atmosphere. The oxygen content of the as-quenched ribbon samples was analyzed to be less than 800 mass ppm by inductively coupled plasma spectroscopy. The influence of oxygen on the transformation behavior can thus be disregarded.<sup>7</sup>

*In situ* x-ray powder diffraction (XRD) measurements were performed at HASYLAB (Hamburg, Germany) on the experimental station Petral using monochromatic synchrotron radiation of 21 keV and a two-dimensional detector. The sample was continuously heated for *in situ* measurements from 300 to 850 K at a rate of 10 K/min under vacuum. EXAFS measurements were performed at the A1 station in transmission geometry. The same heater as in XRD measurement was used for pre-annealing of samples directly on the beamline. Data were taken after cooling down to 300 K with the aim of reducing the temperature-dependent damping of the oscillatory part of the absorption coefficient. Measured spectra were analyzed by standard procedures of data reduction, using the program VIPER.<sup>23</sup> The Fourier transformation (FT) gives a radial distribution function (RDF), modified by the phase shifts due to the absorbing and backscattering atoms. A selected number of shells were backtransformed into k-space. The structural parameters  $N$  (coordination number),  $R$  (interatomic distance), and  $\sigma$  (relative displacement of atoms) were obtained from least squares fitting in k-space, using theoretical phases and amplitude functions calculated by the FEFF-8 code.<sup>24</sup>

Figures 1(a) and 1(b) show XRD patterns of  $\text{Zr}_{70}\text{Cu}_{30}$  and  $\text{Zr}_{70}\text{Cu}_{29}\text{Pd}_1$  at different stages of annealing. Up to 583 K, the patterns of both samples exhibit a broad peak located

<sup>a)</sup> Author to whom correspondence should be addressed; electronic mail: jjiang@fysik.dtu.dk

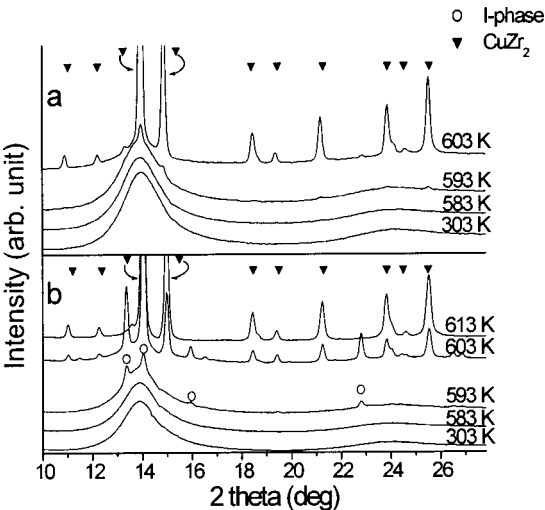


FIG. 1. *In situ* high-temperature XRD patterns of (a)  $\text{Zr}_{70}\text{Cu}_{30}$  and (b)  $\text{Zr}_{70}\text{Cu}_{29}\text{Pd}_1$  ribbon samples using a wavelength of 0.05904 nm.

at  $2\theta \approx 13.8^\circ$  characteristic for the amorphous structure. At 593 K, XRD patterns of  $\text{Zr}_{70}\text{Cu}_{30}$  and  $\text{Zr}_{70}\text{Cu}_{29}\text{Pd}_1$  samples show diffraction peaks which can be indexed as a tetragonal  $\text{CuZr}_2$  phase ( $a=0.322$  nm and  $c=1.118$  nm, space group  $I4/mmm$ ) and an icosahedral quasicrystalline phase (I-phase), respectively. At 603 K, both I-phase and  $\text{CuZr}_2$  phase are observed in  $\text{Zr}_{70}\text{Cu}_{29}\text{Pd}_1$  sample, while a tiny trace of the I-phase ( $2\theta \approx 13.2^\circ$ ,  $16^\circ$ , and  $22.8^\circ$ ) was also present in  $\text{Zr}_{70}\text{Cu}_{30}$  sample. Above 613 K, only the  $\text{CuZr}_2$  phase is detected in both samples. Figure 2 shows schematic drawings of an icosahedral cluster around a Zr atom and the  $\text{CuZr}_2$  lattice, respectively.

Figure 3(a) shows the normalized experimental EXAFS spectra measured at the Zr K edge of  $\text{Zr}_{70}\text{Cu}_{29}\text{Pd}_1$  in the as-prepared state and after pre-annealing at 593 and 773 K. Corresponding FTs are shown in Fig. 3(b). Measured EXAFS signals as well as FTs of the sample annealed at 593 K (where the I-phase was detected by XRD) and as-prepared sample look very similar. This indicates similar local atomic environment around Zr in both stages. Overlapping of two shells in RDF [marked by arrows on Fig. 3(d)] and only one smooth peak in the RDF around Cu atoms (EXAFS signal

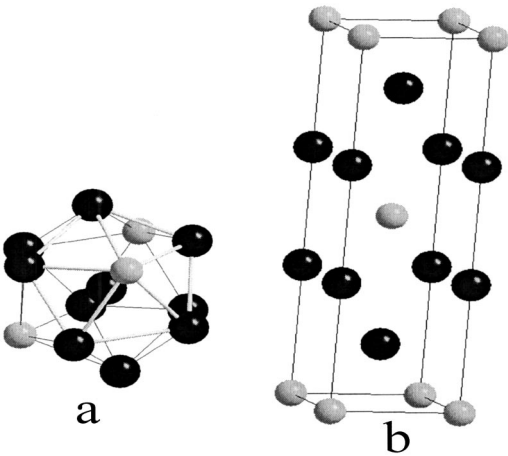


FIG. 2. Schematic drawings of (a) icosahedral cluster and (b) unit cell of tetragonal  $\text{CuZr}_2$  structure with black spheres for Zr atoms and white spheres for Cu atoms.

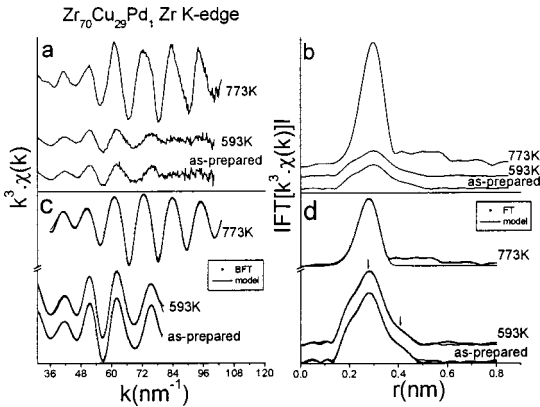


FIG. 3. (a) Experimental  $k^3 \cdot \chi(k)$  for  $\text{Zr}_{70}\text{Cu}_{29}\text{Pd}_1$  alloy in as-prepared stage and after pre-annealing at 593 and 773 K measured above Zr edge, (b) Fourier transforms of (a), (c) Fourier filtered signal (dots) from selected number of shells and simulated EXAFS spectra (line), and (d) Fourier transforms of (c).

measured above Cu edge not shown here) indicate the existence of short-range order around Zr. Saida *et al.*<sup>22</sup> reported a coordination number  $N \approx 12$  around Zr in glassy  $\text{Zr}_{70}\text{Cu}_{30}$ , suggesting the formation of icosahedral configurations around Zr. For calculations a model of icosahedral clusters around the Zr atoms was chosen (Fig. 2). The outer shells of the icosahedral cluster model are composed of Zr and Cu. Despite the fact that 1 at. % of Pd plays an important role in stabilizing the local atomic order Pd was excluded from the model calculations. By using the theoretically calculated amplitude and phase factors spectra taken from as-prepared and pre-annealed (593 K)  $\text{Zr}_{70}\text{Cu}_{29}\text{Pd}_1$  can be fitted. The outline of our fitting procedure is as follows. Two shells in the range of 0.12 to 0.48 nm were back transformed to k-space. Each shell consists of two subshells Zr-Zr and Zr-Cu. The total coordination number in each shell was constrained  $N_{\text{Zr-Zr}} + N_{\text{Zr-Cu}} = 12$ . The structural parameters,  $R_i$ ,  $\sigma_i$  and relative coordination number from each subshell, were obtained by fitting of back Fourier filtered signal. Figures 3(c) and 3(d) show results obtained from the best fitting, refined structural parameters from the fits are listed in Table I. To analyze the EXAFS signal of  $\text{Zr}_{70}\text{Cu}_{29}\text{Pd}_1$  annealed at 773 K (where only  $\text{CuZr}_2$  diffraction peaks were present in XRD), another approach was used. The Zr atom in the tetragonal  $\text{CuZr}_2$  phase is surrounded by four Cu atoms at a distance of 0.288 nm, four Zr atoms at a distance of 0.307 nm and four Zr

TABLE I. Structural parameters for  $\text{Zr}_{70}\text{Cu}_{29}\text{Pd}_1$  and  $\text{Zr}_{70}\text{Cu}_{30}$  samples by using an icosahedral model.

Zr <sub>70</sub> Cu <sub>29</sub> Pd <sub>1</sub> Zr edge							
Annealing temperature [K]	Number of the shell	R [nm]±0.0001		N±0.1		σ [nm]±0.0001	
		Zr-Zr	Zr-Cu	Zr-Zr	Zr-Cu	Zr-Zr	Zr-Cu
300	1	0.2761	0.2798	9.2	2.8	0.0235	0.0145
	2	0.4483	0.4514	7.7	4.3	0.0230	0.0182
593	1	0.2759	0.2795	8.9	3.1	0.0226	0.0158
	2	0.4479	0.4520	7.8	4.2	0.0221	0.0176
Zr <sub>70</sub> Cu <sub>30</sub> Zr edge							
300	1	0.2763	0.2794	9.1	2.9	0.0241	0.0138
	2	0.4479	0.4517	7.9	4.1	0.0226	0.0212

TABLE II. Structural parameters for  $\text{Zr}_{70}\text{Cu}_{29}\text{Pd}_1$  and  $\text{Zr}_{70}\text{Cu}_{30}$  samples by using a  $\text{CuZr}_2$  model.

Annealing temperature [K]	$\text{Zr}_{70}\text{Cu}_{29}\text{Pd}_1$ Zr edge								
	$R$ [nm] $\pm 0.0001$			$N$			$\sigma$ [nm] $\pm 0.0001$		
	Zr-Cu	Zr-Zr	Zr-Zr	Zr-Cu	Zr-Zr	Zr-Zr	Zr-Cu	Zr-Zr	Zr-Zr
773	0.2807	0.3062	0.3190	4	4	4	0.0172	0.0113	0.0103
	$\text{Zr}_{70}\text{Cu}_{30}$ Zr edge								
	$R$ [nm] $\pm 0.0001$			$N$			$\sigma$ [nm] $\pm 0.0001$		
	Zr-Cu	Zr-Zr	Zr-Zr	Zr-Cu	Zr-Zr	Zr-Zr	Zr-Cu	Zr-Zr	Zr-Zr
593	0.2787	0.3074	0.3187	4	4	4	0.0184	0.0128	0.0148
773	0.2807	0.3067	0.3216	4	4	4	0.0171	0.0106	0.0103

atoms at a distance of 0.322 nm. From the  $\text{CuZr}_2$  model new amplitudes and phase factors were calculated. The major peak in the RDF from 0.1 to 0.38 nm was back transformed to  $k$ -space, and the resulting filtered signal was fitted by using coordination number constraints for each subshell. Figures 3(c) and 3(d) show the fit and the structural parameters are listed in Table II. Figure 4(a) shows normalized EXAFS spectra measured at the Zr K edge taken from as-prepared  $\text{Zr}_{70}\text{Cu}_{30}$  and the same sample pre-annealed at 593 and 773 K. The oscillatory signal of as-prepared  $\text{Zr}_{70}\text{Cu}_{30}$  alloy is similar to that of as-prepared  $\text{Zr}_{70}\text{Cu}_{29}\text{Pd}_1$  alloy, however, the signal from  $\text{Zr}_{70}\text{Cu}_{30}$  alloy annealed at 593 K is significantly different (pronounced oscillations of  $k^3 \cdot \chi(k)$  up to 100  $\text{nm}^{-1}$  and almost double amplitude) compared to that of the as-prepared state as well as the signal from  $\text{Zr}_{70}\text{Cu}_{29}\text{Pd}_1$  annealed at the same temperature. Corresponding differences can also be seen after FT of the oscillatory signals to  $r$ -space [Fig. 4(b)]. EXAFS spectra of as-prepared  $\text{Zr}_{70}\text{Cu}_{30}$  were analyzed by the same fitting procedure used for the quasicrystalline  $\text{Zr}_{70}\text{Cu}_{29}\text{Pd}_1$  sample. Spectra from pre-annealed samples were fitted using the procedure for the  $\text{CuZr}_2$  structure. The best fits are shown on Figs. 4(c) and 4(d), and resulting parameters from the fits are listed in Tables I and II. From these examinations, we can summarize that the local atomic environments of the as-quenched  $\text{Zr}_{70}\text{Cu}_{30}$  glassy alloy are similar to those in the as-quenched and annealed at 593 K (I-phase is formed) in the  $\text{Zr}_{70}\text{Cu}_{29}\text{Pd}_1$  glassy alloy, where the corresponding local atomic environments match to the icosahedral local atomic configuration.

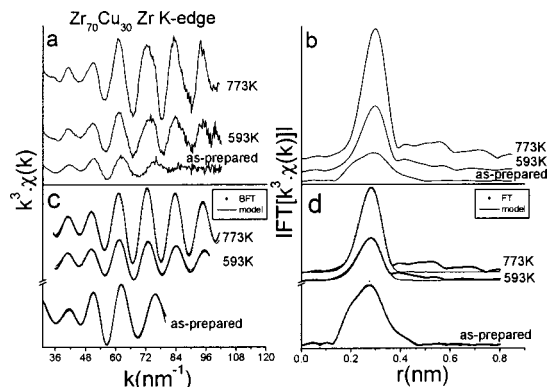


FIG. 4. (a) Experimental  $k^3 \cdot \chi(k)$  for  $\text{Zr}_{70}\text{Cu}_{30}$  alloy in as-prepared stage and after pre-annealing at 593 and 773 K measured above Zr edge, (b) Fourier transforms of (a), (c) Fourier filtered signal (dots) from selected number of shells and simulated EXAFS spectra (line), and (d) Fourier transforms of (c).

These local atomic environments change into the  $\text{CuZr}_2$  structure with annealing at the temperature over 593 K in the  $\text{Zr}_{70}\text{Cu}_{30}$  and at 773 K in the  $\text{Zr}_{70}\text{Cu}_{29}\text{Pd}_1$  glassy alloys, indicating that the local atomic arrangement in the binary composition is more flexible (can more easily adopt stable  $\text{CuZr}_2$  structure) than the alloy containing Pd. By addition of Pd the local icosahedral atomic configuration becomes more rigid, suppressing the redistribution of constituent elements to form the  $\text{CuZr}_2$  phase. Since the supercooled liquid state appears prior to crystallization in these alloys, it is concluded that the formation of icosahedral local structure is supposed to be a dominant factor for the high glass-forming ability; that is, high stability of the supercooled liquid state of the Zr-based glassy alloys.

- <sup>1</sup>U. Köster, J. Meinhardt, S. Roos, and H. Liebertz, Appl. Phys. Lett. **69**, 179 (1996).
- <sup>2</sup>J. Saida, M. Matsushita, and A. Inoue, Appl. Phys. Lett. **77**, 73 (2000).
- <sup>3</sup>B. S. Murty, D. H. Ping, and K. Hono, Appl. Phys. Lett. **77**, 1102 (2000).
- <sup>4</sup>J. Z. Jiang, K. Saksl, J. Saida, A. Inoue, H. Franz, K. Messel, and C. Lathe, Appl. Phys. Lett. **80**, 781 (2002).
- <sup>5</sup>J. Saida, M. Matsushita, C. Li, and A. Inoue, Appl. Phys. Lett. **76**, 3558 (2000).
- <sup>6</sup>S. Yi and D. H. Kim, J. Mater. Res. **15**, 892 (2000).
- <sup>7</sup>B. S. Murty, D. H. Ping, K. Hono, and A. Inoue, Appl. Phys. Lett. **76**, 55 (2000).
- <sup>8</sup>B. S. Murty, D. H. Ping, K. Hono, and A. Inoue, Scr. Mater. **43**, 103 (2000).
- <sup>9</sup>M. Matsushita, J. Saida, C. Li, and A. Inoue, J. Mater. Res. **15**, 1280 (2000).
- <sup>10</sup>J. Eckert, N. Mattern, M. Zinkevitch, and M. Seidel, Mater. Trans., JIM **39**, 623 (1998).
- <sup>11</sup>A. Inoue, J. Saida, M. Matsushita, and T. Sakurai, Mater. Trans., JIM **41**, 362 (2000).
- <sup>12</sup>D. V. Louzguine and A. Inoue, Appl. Phys. Lett. **78**, 1841 (2001).
- <sup>13</sup>L. Q. Xing, J. Eckert, W. Löser, and L. Schultz, Appl. Phys. Lett. **74**, 664 (1999).
- <sup>14</sup>M. W. Chen, T. Zhang, A. Inoue, A. Sakai, and T. Sakurai, Appl. Phys. Lett. **75**, 1697 (1999).
- <sup>15</sup>A. Inoue, T. Zhang, J. Saida, M. Matsushita, M. W. Chen, and T. Sakurai, Mater. Trans., JIM **40**, 1181 (1999).
- <sup>16</sup>J. K. Lee, G. Choi, D. H. Kim, and W. T. Kim, Appl. Phys. Lett. **77**, 978 (2000).
- <sup>17</sup>J. Z. Jiang, A. R. Rasmussen, C. H. Jensen, Y. Lin, and P. L. Hansen, Appl. Phys. Lett. **80**, 2090 (2002).
- <sup>18</sup>J. Z. Jiang, Y. X. Zhuang, H. Rasmussen, J. Saida, and A. Inoue, Phys. Rev. B **64**, 094208 (2001).
- <sup>19</sup>N. Wanderka, M. P. Macht, M. Seidel, S. Mechler, K. Ståhl, and J. Z. Jiang, Appl. Phys. Lett. **77**, 3935 (2000).
- <sup>20</sup>U. Kuhn, J. Eckert, N. Mattern, and L. Schultz, Appl. Phys. Lett. **77**, 3176 (2000).
- <sup>21</sup>J. Saida, N. Matsushita, and A. Inoue, Mater. Trans., JIM **43**, 1937 (2002).
- <sup>22</sup>J. Saida, M. Kasai, E. Matsubara, and A. Inoue, Ann. Chim. Sci. Matér. **27**, 77 (2002).
- <sup>23</sup>K. V. Klementev, J. Phys. D **34**, 209 (2001).
- <sup>24</sup>A. L. Ankudinov, B. Ravel, J. J. Rehr, and S. D. Conradson, Phys. Rev. B **58**, 7565 (1998).